Title: *Drosophila* menthol sensitivity and the Precambrian origins of TRP-dependent chemosensation

Authors and Affiliations:

Nathaniel J. Himmel[1,*], Jamin M. Letcher[1], Akira Sakurai[1], Thomas R. Gray[1], Maggie N. Benson[1], and Daniel N. Cox[1,*]

1 - Neuroscience Institute, Georgia State University, Atlanta, GA 30303

* - Corresponding Authors:

Keywords: TRP channels, chemosensation, nociception, menthol, *Drosophila*, evolution

Authors for Correspondence:

Nathaniel J. Himmel
Neuroscience Institute
Georgia State University
P.O. Box 5030
Atlanta, GA 30302-5030
nhimmel1@student.gsu.edu

Daniel N. Cox
Neuroscience Institute
Georgia State University
P.O. Box 5030
Atlanta, GA 30302-5030
dcox18@gsu.edu

Abstract

Transient receptor potential (TRP) cation channels are highly conserved, polymodal sensors which respond to a wide variety of stimuli. Perhaps most notably, TRP channels serve critical functions in nociception and pain. A growing body of evidence suggests that TRPM (Melastatin) and TRPA (Ankyrin) thermal and electrophile sensitivities predate the protostome-deuterostome split (>550 million years ago). However, TRPM and TRPA channels are also thought to detect modified terpenes (*e.g.*, menthol). Although terpenoids like menthol are thought to be aversive and/or harmful to insects, mechanistic sensitivity studies have been largely restricted to chordates. Furthermore, it is unknown if TRP-menthol sensing is as ancient as thermal and/or electrophile sensitivity. Combining genetic, optical, electrophysiological, behavioural, and phylogenetic approaches, we tested the hypothesis that insect TRP channels play a conserved role in menthol sensing. We found that topical application of menthol to *Drosophila melanogaster* larvae elicits a *Trpm*- and *TrpA1*-dependent nocifensive rolling behaviour, which requires activation of Class IV nociceptor neurons. Further, in characterizing the evolution of TRP channels, we put forth the hypotheses that 3 previously undescribed TRPM channel clades (basal, αTRPM, and βTRPM), as well as TRPs with residues critical for menthol sensing, were present in ancestral bilaterians.

Introduction

Menthol and icilin are often referred to as "cooling agents" – while these chemicals do not physically chill, topical application typically elicits a pleasant cooling sensation in humans [1]. Perhaps owing to its perceived cooling properties, menthol has been used as a topical analgesic, often to reduce the severity of itching and/or burning sensations [2-4]. That said, what is pleasant, harmful, or potentially painful will often be species-dependent. It has been previously reported that menthol affects the behaviour of insects; for example, menthol-infused foods are aversive to *Drosophila melanogaster*, and there is some evidence that menthol functions as an insecticide [5-11]. However, relatively little is known concerning the mechanisms by which insects sense and respond to the cooling agents, as previous studies have focused largely on deuterostomes, and, with respect to molecular determinants among those species, chiefly on terrestrial chordates [12-20]. By extension, it is unknown if possible shared mechanisms have their origins in a common ancestor.

Like many other compounds, menthol and icilin are thought to be detected by TRP channels – primarily TRPM8 and TRPA1 [17, 21, 22]. TRP channels are variably selective cation channels which are differentially gated by a wide variety of thermal, chemical, and mechanical stimuli. It is the multimodal nature of TRPM8 and TRPA1 – in humans constituted by at least menthol, icilin, and cold sensing – which partly underlies the similar phenomenological character (*i.e.*, cooling) associated with these very different stimuli [22-24].

The chordate TRPM (TRP Melastatin) family is typically divided into 8 distinct paralogues (TRPM1-TRPM8) thought to have emerged sometime prior to the divergence of tetrapods and fish (although fish are thought to have lost their TRPM8 orthologue) [25]. TRPM8 is multimodal, responding to cold, menthol, and in mammals, icilin [22, 26]. It has been suggested that menthol directly binds with the TRPM8 Voltage Sensor-Like Domain (VSLD), and gating requires interactions between this domain, bound menthol molecules, and the highly conserved C-terminal TRP domain [13, 20]. TRPM8-menthol gating has

1

47 been well characterized in mammalian channels, and a number of critical amino acid
48 residues have been identified in both the VSLD and the TRP domain [12, 14, 16, 19, 20].

49   In contrast to the TRPM family, the chordate TRPA (TRP Ankyrin) family is very
50 small, typically containing only a single member, TRPA1 [27, 28]. TRPA1 is a polymodal
51 nociceptor involved in the detection of noxious cold, noxious heat, menthol, icilin, and
52 electrophilic chemicals such as allyl isothiocyanate (AITC, found in mustard oil and wasabi)
53 [21, 24, 29, 30]. It has been suggested that TRPA1 menthol sensitivity is linked to specific
54 serine and threonine residues found in transmembrane segment 5, and that several nearby
55 residues are responsible for species-specific TRPA1-menthol interactions [31].

56   Insects lack a true TRPM8 orthologue. In fact, the *Drosophila* genomes contains
57 only a single TRPM family gene, *Trpm* (**Figure 1, top**) [32]. While separated by several
58 gene duplication events and more than 550 million years of evolution, *Drosophila* Trpm and
59 its chordate counterpart, TRPM8, are both involved in cold sensing [33]. With respect to
60 TRPAs, the *Drosophila* genome encodes 4 TRPA family genes (**Figure 1, bottom**): *TrpA1*
61 (the homologue to chordate *TRPA1*), *painless* (*pain*), *water witch* (*wtrw*), and *pyrexia* (*pyx*).
62 Like vertebrate TRPA1, *Drosophila* TrpA1 has been implicated in high-temperature and
63 chemical nociception [27, 33-37].

64   TRPA1 high-temperature and electrophile sensitivities are present in both
65 protostomes and deuterostomes [27, 36-45]. While current evidence suggests – despite
66 some controversy – that TRPA1 cold sensitivity evolved relatively recently, perhaps among
67 early synapsids (<300 mya) [46-48], TRPM cold sensitivity is conserved in insects [33]. As
68 such, a growing body of evidence suggests that TRP channel thermal and electrophile
69 sensitivity may have a common origin predating the protostome-deuterostome split (>550
70 mya). However, it remains unknown if TRPA- and TRPM-dependent menthol sensitivity is
71 equally ancient.

72   In order to further elucidate the evolutionary history of TRPM and TRPA channels,
73 we explored the mechanisms by which *Drosophila* senses and responds to cooling agents.
74 Herein, we report that topical menthol application elicits a dose-dependent nocifensive
75 rolling behaviour in *Drosophila*. Further, we use a suite of genetic, optical,
76 electrophysiological, and behavioural approaches to demonstrate that the menthol-evoked
77 response is *Trpm*- and *TrpA1*-dependent, and acts via Class IV (CIV) nociceptors. Finally,
78 in light of these findings, we assess the evolutionary histories and sequence homologies of
79 TRPM and TRPA channels. In doing so, we characterize several putative TRPM and TRPA
80 channels in *Acropora digitifera* (coral), *Strongylocentrotus purpuratus* (purple sea urchin),
81 *Octopus bimaculoides* (California two-spot octopus), *Priapulus caudatus* (penis worm), and
82 *Aplysia californica* (California sea hare), as well as outline the discovery of three previously
83 undescribed TRPM channel clades (basal TRPMs, αTRPMs, and βTRPMs), which we
84 hypothesize were present in the last common bilaterian ancestor, Urbilateria. The results of
85 these studies add to a growing body of evidence suggesting that chemosensation and
86 nociception have functional origins in the Precambrian world [49].

87

Materials & Methods

88

Animals

89

90 All *Drosophila melanogaster* stocks were maintained at 24°C under a 12:12 light:dark cycle.
91 In order to accelerate development, genetic crosses (and relevant controls) were raised for

2

92   5 days at 29°C under a 12:12 light:dark cycle. Wandering 3rd instar larvae were used for all
93   experiments. The OregonR (ORR) strain was used to assess wild-type behaviour, and,
94   where appropriate, the w^{1118} strain and outcrossed parental strains were used as genetic
95   background controls. Transgenic and mutant strains included: $Trpm^2$ and $wtrw^1$ (gifts of K.
96   Venkatachalam); $TrpA1^{W903*}$ and $TrpA1^1$ (gifts of W. D. Tracey); pyx^3, $pain^{70}$, and $Trpm$
97   deficiency $Df(2R)XTE$-11 (gifts of M. J. Galko); $GAL4^{GMR57C10}$ (pan-neuronal driver, BDSC
98   #39171); $GAL4^{ppk}$ (Class IV driver, BDSC #32079); UAS-$CaMPARI$ (BDSC #58763); UAS-
99   $TeTxLC$ (active tetanus toxin, BDSC #28837); UAS-IMP-TNT^{VI-A} (inactive tetanus toxin,
100 BDSC #28840); UAS-$TrpA1$-$RNAi$ 1 (BDSC #31384); UAS-$TrpA1$-$RNAi$ 2 (BDSC #66905);
101 UAS-$Trpm$-$RNAi$ 1 (BDSC #31672); and UAS-$Trpm$-$RNAi$ 2 (BDSC #31291).

102

Behaviour

104 L(-)-menthol (Acros Organics) and icilin (Tocris Bioscience) were suspended in liquid DMSO
105 at various concentrations. Solutions were discarded after 24 hours. Individual larval
106 subjects were placed in a well of a glass 9-well plate, and 10µL of solution was delivered to
107 the well via micropipette. Subjects were observed for 60 seconds and their behaviours
108 recorded. In order to increase subject-background contrast in the representative
109 images/videos, animals were left to freely locomote on a moist black arena, and menthol
110 was applied as above.

111

CaMPARI-based Ca^{2+} analyses

113 UAS-$CaMPARI$ expression was driven via $GAL4^{GMR57C10}$. Live, freely behaving larvae were
114 exposed to 8% menthol or vehicle as described above. Photoconverting light was delivered
115 under a Zeis AxioZoom V16 microscope as previously described [50, 51]. Larvae were
116 subsequently placed in 1 drop of 1:5 diethyl ether:halocarbon oil and secured between a
117 slide and slide cover. Class IV neurons were imaged via a Zeiss LSM780 confocal
118 microscope, and the resulting z-stacks were volume rendered as two-dimensional maximum
119 intensity projections. Red and green fluorescence intensity was assessed using the FIJI
120 distribution of ImageJ software.

121

Electrophysiology

123 To record single-unit spiking activity of Class IV neurons, we first prepared fillet preparations
124 from $GAL4^{ppk}$>UAS-$mCD8$::GFP larvae. Larvae were placed in a petri dish lined with
125 Sylgard® 184 (Dow Corning, Midland, MI) filled with HL-3 saline. The ventral body wall was
126 cut open with fine scissors, and all muscles were carefully removed with a polished tungsten
127 needle and scissors. The preparation was then constantly superfused with HL-3 saline at a
128 rate of 1 mL/min at room temperature, and allowed to rest for more than 1 hour before
129 recording. Menthol was first dissolved in DMSO at a concentration of 500 mM and then
130 diluted in HL-3 saline to a final concentration 0.5 mM. Menthol was bath-applied to the
131 specimen through superfusion. Extracellular recordings were made with a macropatch
132 pipette (tip diameter = 5-10 µm) connected to the headstage of a patch-clamp amplifier
133 (AxoPatch200B, Molecular Devices, Sunnyvale, CA). Gentle suction was applied to draw
134 the soma and a small portion of neurite into the pipette. The amplifier was set to the track
135 mode to record neuronal spikes. The output signals from the amplifier were digitized at a

136 sampling frequency of 10 kHz using a Micro1401 A/D converter (Cambridge Electronic
137 Design, Cambridge, UK) and acquired into a laptop computer running Windows 10 with
138 Spike2 software ver. 8 (Cambridge Electric Design, Cambridge, UK). Average spike
139 frequency was measured in a 30 sec time window during baseline control conditions,
140 superfusion of vehicle, and superfusion of menthol.

141

Phylogenetics

143 Amino acid sequences for previously characterized TRP channels were collected from the
144 following databases: JGI Genome (*Monosiga brevicollis*, *Nematostella vectensis*, and
145 *Daphnia pulex*), Ensembl (*Danio rerio*, *Gallus gallus*, and *Strigamia maritima*), NCBI (*Hydra*
146 *vulgaris*, *Homo sapiens*, *Mus musculus*, *Apis mellifera*, and *Galendromus occidentalis*),
147 WormBase (*Caenorhabditis elegans*), or FlyBase (*Drosophila melanogaster*). *Panulirus*
148 *argus* sequences were collected from [52]. In order to identify novel TRPM and TRPA
149 channels, publically available protein models based on genomic and/or transcriptomic
150 sequences for *Acropora digitifera* [53], *Strongylocentrotus purpuratus* [54, 55], *Octopus*
151 *bimaculoides* [56], *Priapulus caudatus* (BioProject PRJNA20497, GenBank
152 AXZU00000000.2), and *Aplysia californica* (BioProject, PRJNA209509, GenBank
153 AASC00000000.3) were pBLASTed [57] against *D. melanogaster* TRP sequences.
154 Sequences >200aa in length and with an E-value <1E-30 were retained and subsequently
155 analyzed via InterProScan [58]. Sequences which had predicted transmembrane segments
156 and characteristic Ankyrin repeats (for TRPAs) were retained. Accession numbers are
157 available in the supplementary material (**Table S1**).

158 Amino acid sequences were MUSCLE [59] aligned in MEGA7 [60]. Poorly aligned regions
159 and spurious sequences were identified and trimmed using automated methods packaged
160 with TrimAl [61]. As TRPA Ankyrin repeats were generally poorly aligned, they were
161 manually removed prior to automated trimming by excluding everything N-terminal of 20aa
162 before the start of predicted transmembrane segment 1. IQ-Tree was then used to perform
163 a composition chi^2 test in order to assess sequence homogeneity within TRP subfamilies
164 [62]. Due to extreme divergence, and in order to minimize possible topology disruptions
165 due to long branch attraction [63-65], *P. argus* TRPMm, TRPA-like1, and TRPA5-like1, and
166 *C. elegans* TRPA-2 were excluded from final analyses; each failed the composition chi^2 test
167 and introduced extremely long branches with weak support in a first-pass analysis. Final,
168 trimmed alignments were used to generate phylogenetic trees. Bayesian trees were
169 constructed in MrBayes (version 3.2.6) using a mixed amino acid substitution model and a
170 gamma distributed rate of variation [66, 67]. Two independent MCMC analyses (initial
171 settings: 1,000,000 chains with sampling every 10) were run until convergence (<0.05).
172 25% of the chain was considered burn-in and discarded. Maximum likelihood trees were
173 constructed in IQ-Tree using an amino acid substitution model automatically selected by
174 ModelFinder [68]. Ultrafast bootstrapping (2000 bootstraps) was also performed in IQ-Tree
175 [69]. Trees were visualized and edited in iTOL [70] and Adobe Illustrator CS6. Branches
176 with low support (posterior probability <0.7 or bootstrap <70) were considered unresolved,
177 and were collapsed to polytomies in the final trees. Ancestral sequence predictions were
178 made in MEGA7 using the maximum likelihood approach against previously generated
179 alignments and Bayesian trees [71].

180

181

Statistical analyses

Population proportions are presented as % ± standard error of the proportion (SEP); differences in proportion were assessed using a generalized linear model with a logit link and a binomial error distribution, and pairwise comparisons were made using the lsmeans R package [72] and the Tukey method for multiple comparisons. CaMPARI photoconversion, spike frequency, and latency measures are presented as mean ± standard error of the mean (SEM); differences were assessed in GraphPad PRISM (GraphPad Software, La Jolla, California, USA) by unpaired t-test or ANOVA with Dunnett's *post-hoc* test. Asterisk (*) indicates statistical significance p<0.05, with significant p-values (as compared to wild-type or appropriate control) listed in the associated figure legend.

Results

Menthol elicits *Trpm*- and *TrpA1*-dependent nocifensive rolling in *Drosophila* larvae

Vehicle (DMSO), menthol, or icilin was topically applied to freely behaving *Drosophila melanogaster* larvae, and their behaviour recorded (10μL, delivered via micropipette). Mentholated solutions elicited a stereotyped rolling behavior, identical to a previously described [73, 74] nocifensive response (**Figure 2A; Movie S1**). The proportion of animals which responded to menthol increased with higher menthol concentrations (**Figure 2B**). In contrast, treatment with DMSO (**Figure 2B, vehicle; Movie S2**) or icilin (**Figure 2B; Movie S3**) did not elicit rolling.

Given TRP-dependent mechanisms of menthol sensing in vertebrates, we hypothesized that menthol-evoked rolling requires TRPM and TRPA channels. To test this, we assessed the behaviour of whole-animal *Trpm*, *TrpA1, pyx, pain,* and *wtrw* mutants. Compared to control, a significantly smaller proportion of homozygous *TrpA1* and *Trpm* mutants rolled in response to menthol (**Figure 2C**). Additionally, we observed a significantly increased latency to roll for those *TrpA1*^{W903*} mutants that did respond (**Figure 2D**). In contrast, *pain* mutation sensitized larvae to menthol – homozygous *pain* mutants rolled with severely decreased latency, and many rolled immediately following menthol application (**Figure 2D**). Given that *painless* mutants could be sensitized to the point of immediately rolling following menthol application, it appears likely that menthol was rapidly delivered across the cuticle.

As *TrpA1* and *Trpm* were both required for the menthol-evoked response, mutations were tested combinatorially. While heterozygous *TrpA1* (*TrpA1*^{W903*}/+ and *TrpA1*^{1}/+) and *Trpm* (*Trpm*^{2}/+ and *Trpm* df/+) mutants had no significant behavioural defects, transheterozygous (*TrpA1*^{W903*}/+;*Trpm*^{2}/+) mutants exhibited significantly inhibited menthol-evoked rolling, indicating that these channels genetically interact in menthol sensing (**Figure 2C**).

Class IV nociceptors mediate menthol-evoked rolling

Drosophila larvae have two known classes of peripheral nociceptors: multidendritic (md) Class III neurons are cold nociceptors and innocuous touch mechanosensors, whereas md Class IV (CIV) neurons are polymodal nociceptors which detect noxious heat, mechanical insults, and short-wavelength light [33, 34, 74-78]. As rolling behaviour has been previously associated with CIV nociceptor activation, we hypothesized that menthol-

226 evoked rolling requires CIV activation. In order to assess activation patterns *in vivo*, the
227 *GAL4-UAS* system was used to drive neuronal expression of CaMPARI [79], a genetically
228 encoded Ca^{2+} indicator. Live, freely behaving transgenic animals were exposed to menthol
229 or vehicle, as above. The level of CIV neural activation was assessed *post-hoc,* in live
230 animals, as a green-to-red shift in CaMPARI fluorescence, which occurs in the presence of
231 violet light as a function of increases in intracellular Ca^{2+} concentration. CaMPARI analyses
232 revealed significant activation of CIV nociceptors in response to menthol, relative to vehicle
233 control (**Figure 3A**). To directly assess menthol-evoked activation of CIV neurons, we
234 performed single-unit electrophysiological recordings of CIV neurons. Electrophysiological
235 recordings demonstrate that superfusion of menthol significantly increases spike frequency
236 in CIV neurons relative to controls (**Figure 3B**).

237 In order to test the necessity of CIV neurons for menthol-evoked rolling, genetically
238 encoded active tetanus toxin (TNT) was used to block synaptic transmission in CIV
239 neurons. GAL4[ppk]-driven, CIV-specific expression of TNT completely ablated menthol-
240 evoked rolling (**Figure 4**).

241 In light of TRP mutant and CIV TNT phenotypes, we hypothesized that menthol-
242 evoked behaviour may be dependent on TrpA1 and/or Trpm function in CIV nociceptors.
243 We previously demonstrated that *TrpA1* and *Trpm* transcripts are detectibly expressed in
244 CIV nociceptors ([80], GEO: GSE46154). Consistent with these data, CIV-targeted, RNAi-
245 mediated knockdown of *Trpm* or *TrpA1* strongly inhibited menthol-evoked rolling (**Figure 4**),
246 supporting a functional role for these TRP channels in CIV-mediated menthol sensing.

247

Residues critical to menthol sensing were likely present in ancestral bilaterian channels

250 A number of specific amino acid residues have been associated with menthol
251 sensitivity in mammalian TRPM [12, 14, 16, 19, 20] and TRPA [31] channels. Phylogenetic
252 and sequence analyses were performed in order to assess how well conserved these
253 residues are across taxa, and to infer their evolutionary history. The amino acid sequences
254 for 69 TRPM channels and 56 TRPA channels (**Table S1**) were used to generate
255 phylogenetic trees by both Bayesian and maximum likelihood approaches. Trees were
256 constructed using previously and newly characterized TRP sequences across a variety of
257 metazoan species, with a chaonoflagellate (*Monosiga brevicollis*) outgroup (**Figure 5A**).
258 Both methods produced trees with largely consistent topologies (**Figures S1-S4**).

259 It has been previously noted that several species express TRPM-like channels which
260 cluster independent of, or differ greatly from, other chordate and/or insect TRPMs [28, 52,
261 81]. In accordance with this, the consensus TRPM phylogeny shows a group of protostome
262 TRPMs located basally, near chaonoflagellate TRPMs (**Figure 5B, green**). Previously
263 published phylogenies have shown most arthropod TRPMs to be most closely related to
264 chordate TRPMs 1, 3, 6, and 7, yet this relationship has not yet been formally discussed
265 [25, 28]. These trees demonstrate that non-basal TRPM channels group into two
266 monophyletic clades (designated αTRPM and βTRPM), which collectively constitute all
267 other analyzed TRPM channels (**Figure 5B, red and blue**). Each clade contains both
268 protostome and deuterostome TRPMs and is rooted in cnidarian TRPMs, indicating that
269 these two clades may have existed prior to the protostome-deuterostome split. The
270 topology of these trees is consistent with a hypothesis that at least three distinct TRPM
271 channels (designated basal TRPM, αTRPM, and βTRPM) predate the last common

6

272 bilaterian ancestor, Urbilateria. Further, this hypothesis is compatible with previously
273 formulated hypotheses regarding the independent diversification of chordate TRPM
274 channels [25, 28, 32].

275   As both α- and βTRPMs have been implicated in menthol sensing, ancestral
276 sequence predictions were generated for ancestral bilaterian α- and βTRPM. Four TRPM8
277 residues – Y745, R842, Y1005, and L1009 (**Figure 5D, black arrows**) – have been
278 identified as critical to vertebrate menthol sensing [20]. Three of these residues, Y745,
279 R842, and Y1005, are conserved in *Drosophila*, and ancestral sequence predictions
280 suggest with high confidence that they are conserved from a common ancestral bilaterian
281 sequence (**Figure 5D, bottom**). The only site which differs from chordate TRPM8 is a
282 predicted ancestral proline in place of L1009; proline, however, is more common at this site
283 across TRPM channels, including in *Drosophila*, and previous work has shown that L1009P
284 substitution in mouse TRPM8 does not affect menthol sensitivity [12].

285   For TRPAs, both previously characterized clades – TRPA1 and the "basal" clade
286 (**Figure 5C, orange and dark grey**) – formed as expected, and conformed to other
287 published topologies [7, 27, 28, 32]. Although the term "basal" has been used to describe
288 other TRPAs, Peng, Shi, and Kadowaki have suggested that the TRPA1 clade is the most
289 ancestral [28]. This analysis does not clearly support nor undermine this hypothesis. What
290 is clear, however, is that the TRPA1 clade predates the protostome-deuterostome split.

291   Previous work has shown that the TRPA1 pore region is important to mammalian
292 menthol sensitivity. Serine and threonine residues in TM5 are thought to be most critical to
293 menthol sensitivity (**Figure 5E, black arrows**), and a variety of others (**Figure 5E, white
294 arrows**) are associated with species-specific differences in menthol sensitivity [31]. These
295 regions are generally poorly conserved between mammals and other species (**Figure 5E,
296 top**), including other chordates (e.g., *Gallus gallus*). In contrast to TRPM conservation,
297 fewer critical TRPA1 residues appear to be consistently conserved from a common
298 bilaterian ancestor, and there is substantially less certainty as to the identity of these
299 ancestral sequences (**Figure 5E, bottom**).

Discussion

TRP-dependent transduction and menthol sensing in *Drosophila*

302   We have demonstrated that *Drosophila* larvae execute a dose-dependent, menthol-
303 evoked, aversive rolling response consistent with the nocifensive behaviour displayed in
304 response to noxious heat and mechanical insult. Cellularly, menthol exposure activates CIV
305 nociceptors, and blocking synaptic transmission in these neurons inhibits menthol-evoked
306 rolling. Molecularly, TrpA1 and Trpm are required for menthol-induced aversive behaviour,
307 and genetically interact in this capacity.

308   Curiously, it has been previously reported that *Drosophila* TrpA1 does not directly
309 gate in response to menthol [31]. The study in question, however, used lower
310 concentrations of menthol applied to channels expressed *in vitro*. These sorts of
311 discrepancies are not uncommon in studies of other TRPA1 modalities, and there are
312 similar conflicting reports concerning TRPA1's role in cold nociception: some groups report
313 that TRPA1 acts as a direct cold sensor, others state it responds to an indirect, cold-
314 associated factor (reactive oxygen species and/or intracellular Ca^{2+}), while others claim it
315 responds only to innocuous cooling, or does not respond to cold at all [47, 82-86]; some
316 isoforms of TRPA1 have been shown to directly gate in response to noxious high

7

317 temperatures, yet high temperature nociception can be rescued by heat-insensitive isoforms
318 [37]; and there is still debate as to whether or not TRPA1 functions similarly *in vivo* and *in*
319 *vitro* [46]. Further, TRPA1s are differentially activated and/or inhibited by menthol, across
320 species, across concentrations [41, 47]. It is therefore unsurprising, if no less puzzling, that
321 *Drosophila TrpA1* is required for menthol detection *in vivo*, yet the channel does not gate in
322 response to relatively low concentrations of menthol *in vitro*. Instead, these and other
323 findings suggest that we may not fully understand how TRPA1 functions, and that it may not
324 be a simple sensor which directly responds to an incredibly wide variety of stimuli.

325 Moreover, although menthol and TRPA/TRPM interactions are most frequently
326 studied, menthol is likely to be very promiscuous with respect to which channels it activates.
327 Reports suggest that menthol activates, potentiates, or inhibits voltage-gated Na^+ channels,
328 L-type voltage-gated Ca^{2+} channels, the cystic fibrosis transmembrane conductance
329 regulator, mouse TRPV3, TRPL, a wide variety of Ca^{2+}-dependent channels, as well as
330 GABA, serotonin, and acetylcholine receptors [7, 87-91]. Another notable player is the
331 hymenopteran specific TRPA (HsTRPA), which is more closely related to painless than to
332 TRPA1 (**Figure 5C, dark grey**). HsTRPA1 thermal sensitivity is depressed by application
333 of menthol [7]. Given that *painless* mutants are hypersensitive to menthol (**Figure 2C**), the
334 so-called basal TRPAs may be complex mediators of chemo-sensitivity, rather than simple
335 sensors. Currently, the menthol-specific ligand-binding and gating mechanisms of most
336 receptors are not as well understood as those of chordate TRPA1 and TRPM8. However,
337 these mechanisms are no doubt important, perhaps to species-specific behavioral
338 responses, or to menthol's purported analgesic effect [2-4, 88]. Future studies will need to
339 investigate not only how other channels function in menthol sensing, but how they might
340 interact with channels with incompletely understood activation properties (*e.g.*, TRPA1), as
341 these interactions may explain differences in menthol-evoked activity *in vivo* and *in vitro*.

342

TRP channels and the evolution of chemical nociception

344 Phylogenetic analyses have revealed that 3 TRPM clades – designated basal,
345 αTRPM, and βTRPM – and the TRPA1 clade, likely predate the protostome-deuterostome
346 split. Further, many TRPM and TRPA1 residues critical to menthol sensing are conserved
347 from ancestral bilaterian channels (although more variably so for TRPA1s). That residues
348 critical to menthol sensing may predate the protostome-deuterostome split influences how
349 we may understand the evolution of menthol production and avoidance. There is some
350 evidence that menthol may be lethal to several insect species [10, 11], including *D.*
351 *melanogaster* [9]; as such, the ability to sense and respond to menthol may be adaptive.
352 Given that there is considerable latency to roll in response to menthol (**Figure 2D**), it is
353 unclear if the aversive rolling behaviour is protective. Menthol sensing may be more
354 important for adult females, which rather carefully select egg-laying sites and show aversion
355 toward mentholated food [5]. Yet residues critical to menthol sensitivity substantially
356 predate the emergence of Lamiaceae, the family of angiosperms that most notably produce
357 menthol [92, 93]. This appears consistent with early plants evolving menthol (or more
358 broadly, terpene) production in order to repel animals, rather than early animal TRPs
359 evolving menthol sensitivity in order to avoid certain plants. It is possible that animal TRP
360 channels maintained menthol sensitivity since well before terrestrial animals encountered
361 menthol producers, much like how mammalian TRP channels are sensitive to icilin, which is
362 not known to be naturally occurring [1, 16, 84, 94]. Pinpointing the exact origins of these
363 abilities requires additional studies, in particular studies involving more basal (*e.g.*

8

364 Xenacoelomorpha) and non-bilaterian species. Yet, it is conceivable that the functional
365 capacity of these channels evolved in, or prior to, a common bilaterian ancestor, which
366 inhabited a very different environment than extant terrestrial animals [95].

367 The structure of the urbilaterian nervous system is still under considerable debate
368 [96-100]. However, given that TRP channels function in similar ways, in similar subsets of
369 neurons, across taxa, it seems increasingly likely that ancestral TRP channels were
370 expressed in some form of urbilaterian neural tissues, and that these tissues responded to
371 external cues. Still, the function of conserved, menthol-associated residues in ancestral
372 TRPs remains mysterious. However, while menthol production appears to be restricted to
373 plants, terpene production (and more broadly, volatile organic compound production) is far
374 more widespread. For example, volatile organic producers include plants, insects, protists,
375 bacteria, and fungi [101], which have been hypothesized to utilize volatile organic
376 compounds in forms of microbial communication [102]. With this in mind, and concerning
377 terpene sensing by early metazoan TRPs, one plausible hypothesis is that TRP-terpene
378 sensitivity emerged as an early method of communication. Alternatively (or perhaps as sub-
379 hypotheses), TRP-terpene sensing may have been employed as a mechanism by which to
380 identify appropriate food sources, or to signal potential danger, thereby avoiding damage
381 from predation or infection – perhaps an early form of early nociception.

382

Conclusion

384 Herein, we have described cellular and molecular mechanisms by which *Drosophila*
385 *melanogaster* responds to menthol. Phylogenetic analyses revealed that extant TRPM
386 channels are descended from 3 ancestral clades (basal, αTRPM, and βTRPM), and that
387 several residues critical to menthol sensing are conserved from common TRPM and TRPA1
388 ancestors. Collectively, these findings suggest that bilaterian menthol sensing has its
389 origins in a common ancestor, and more broadly, contribute to a body of evidence
390 suggesting that the mechanisms underlying TRP function and chemical nociception are
391 ancient and highly conserved.

392

Acknowledgements

401

Authors' Contributions

403 Conceptualization and experimental design, NJH, JML, AS, and DNC; genetics, NJH and
404 JML; behaviour assays, NJH, JML, MNB; CaMPARI microscopy, NJH and TRG;
405 electrophysiology, AS; phylogenetic and sequence analyses, NJH; statistical analyses, NJH;
406 wrote the original manuscript, NJH; critically analysed and edited the manuscript, NJH, JML,

9

407 AS, TRG, MNB and DNC; approved the final draft, NJH, JML, AS, TRG, MNB, and DNC;
408 funding acquisition, NJH and DNC.

409

Figure Legends

411 **Figure 1.** The *Drosophila melanogaster* (Dm) genome encodes 1 TRPM (Trpm) and 4
412 TRPA (TrpA1, painless, pyrexia, and water witch) channels. Mid-point rooted tree of
413 *Drosophila* (Dm) and human (Hs) TRPMs and TRPAs.

414 **Figure 2.** *Drosophila* larvae exhibit nocifensive rolling in response to menthol. (**A**) Menthol-
415 evoked rolling. Top, cartoon. Bottom, video stills. (**B**) Cumulative proportion of wild-type
416 rollers in response to menthol. The rolling response increased at higher menthol
417 concentrations. Cumulative proportion ± SEP. n=30 for each condition. (**C**) Proportion of
418 rollers in response to 8% menthol. Compared to wild-type, fewer *TrpA1* and *Trpm* mutants
419 rolled in response to menthol (*TrpA1^{W903*}*, p=0.0221; *TrpA1^1*, p=0.0479; *Trpm^2*, p=0.0221;
420 *Trpm^2*/Trpm df, p=0.0221). *Trpm* and *TrpA1* are haplosufficient for menthol sensitivity, but
421 fewer transheterozygous mutants rolled in response to menthol (p=0.0090). Proportions
422 represented as % rollers ± SEP. n=30 for each condition. (**D**) Latency to roll in response to
423 8% menthol. *painless* mutation sensitized rollers (p=0.0006), while *TrpA1^{W903*}* mutation
424 desensitized rollers (p=0.0388). Latency represented as time to roll in seconds ± SEM. n
425 proportional to % rollers, where initial sample size was 30.

426 **Figure 3.** Menthol exposure activates Class IV (CIV) nociceptors. (**A**) (left) Representative
427 CIV CaMPARI photoconversion visualized using a 16-color lookup table. (right) CIV
428 neurons were significantly activated by menthol, as compared to control (p<0.0001).
429 Quantification of CaMPARI photoconversion by F_{red}/F_{green} CaMPARI fluorescence
430 intensities. Photoconversion presented as mean ± SEM. n=18 for each condition. (**B**) (left)
431 Representative CIV single-unit recordings, with insets showing menthol-evoked spiking
432 activity. (right) Menthol superfusion elicited significantly increased average spike frequency
433 in CIV neurons (p=0.0001). Average frequency in Hz ± SEM. Saline control, n=18; DMSO
434 control, n=6; menthol, n=15.

435 **Figure 4**. The TRP-dependent menthol response operates via CIV neurons. Silencing
436 neural transmission in CIV neurons with active tetanus toxin (TNT) completely ablated the
437 menthol response, while CIV-driven expression of inactive TNT did not significantly affect
438 the rolling response. CIV-specific, RNAi-mediated knockdown using two independent
439 transgenes for *TrpA1* and *Trpm* resulted in fewer animals rolling in response to menthol, as
440 compared to control (*TrpA1* RNAi 1, p=0.0032; *TrpA1* RNAi *2*, p=0.0018; *Trpm* RNAi 1,
441 p=0.0032; and *Trpm* RNAi 2, p=0.0032). Proportions represented as % ± SEP. n=30 for
442 each condition.

443 **Figure 5.** The evolutionary history of TRPM and TRPA channels, and of residues critical to
444 menthol sensing. (**A**) (left) Cladogram of species used in analysis. Asterisk (*) indicates that
445 one or more previously known sequences were discarded due to extreme divergence, as
446 described in the Materials & Methods and Supplementary Materials. All sequence
447 accession numbers are available in the Supplementary Materials. (right) Domains
448 previously identified as critical to menthol sensing. (**B**) Bayesian consensus tree for TRPM
449 channels. Posterior probabilities are indicated for each internal branch. Branches with a
450 posterior probability <0.70 were collapsed. For aesthetic purposes, branch lengths were
451 ignored when generating this figure. Trees with branch lengths to scale are available in the

10

452 Supplementary Materials. Green, basal clade; red, αTRPM clade; blue, βTRPM clade. (**C**)

453 Bayesian consensus tree for TRPA channels, as in B. Orange, TRPA1 clade; grey, other

454 TRPAs; dark grey, clade previously described as "basal." (**D**) Alignment for select TRPM

455 sequences and ancestral sequence estimations. Black arrows indicate previously identified

456 critical residue site. % values represent probability of amino acid at the indicated site, at the

457 colour-coded node. (**E**) Alignment for select TRPA sequences and ancestral sequence

458 estimations, as in D. White arrows indicate residues associated with species-specific

459 menthol responses, in mammals. Question mark (?) indicates that no single amino acid

460 was predicted with >50% inferred likelihood.

11

References

461

462 [1] Wei, E. T. & Seid, D. A. 1983 AG-3–5: a chemical producing sensations of cold. *Journal*
463 *of Pharmacy and Pharmacology* **35**, 110-112. (DOI:10.1111/j.2042-7158.1983.tb04279.x).

464 [2] de Souza Romaneli, R., Boaratti André, Z., Tellechea Rodrigues, A., de Almeida ueiroz
465 Daniel, M., Khan Kifayat, U., Nascimento Thiago Matias, T. & Fernandes João Batista, K.
466 2018 Efficacy of Benzocaine, Eugenol and Menthol as Anesthetics for Freshwater Angelfish
467 (*Pterophyllum scalare*). *Journal of Aquatic Animal Health* **0**. (DOI:10.1002/aah.10030).

468 [3] Liu, B. & Jordt, S.-E. 2018 Cooling the Itch via TRPM8. *Journal of Investigative*
469 *Dermatology* **138**, 1254-1256. (DOI:https://doi.org/10.1016/j.jid.2018.01.020).

470 [4] Ton, H. T., Phan, T. X., Abramyan, A. M., Shi, L. & Ahern, G. P. 2017 Identification of a
471 putative binding site critical for general anesthetic activation of TRPA1. *Proceedings of the*
472 *National Academy of Sciences of the United States of America* **114**, 3762-3767.
473 (DOI:10.1073/pnas.1618144114).

474 [5] Abed-Vieillard, D. & Cortot, J. 2016 When Choice Makes Sense: Menthol Influence on
475 Mating, Oviposition and Fecundity in *Drosophila melanogaster*. *Frontiers in Integrative*
476 *Neuroscience* **10**, 5. (DOI:10.3389/fnint.2016.00005).

477 [6] Abed-Vieillard, D., Cortot, J., Everaerts, C. & Ferveur, J.-F. 2014 Choice alters
478 *Drosophila* oviposition site preference on menthol. *Biology Open* **3**, 22-28.
479 (DOI:10.1242/bio.20136973).

480 [7] Kohno, K., Sokabe, T., Tominaga, M. & Kadowaki, T. 2010 Honey Bee
481 Thermal/Chemical Sensor, AmHsTRPA, Reveals Neofunctionalization and Loss of
482 Transient Receptor Potential Channel Genes. *The Journal of Neuroscience* **30**, 12219.
483 (DOI:10.1523/JNEUROSCI.2001-10.2010).

484 [8] Maliszewska, J., Jankowska, M., Kletkiewicz, H., Stankiewicz, M. & Rogalska, J. 2018
485 Effect of Capsaicin and Other Thermo-TRP Agonists on Thermoregulatory Processes in the
486 American Cockroach. *Molecules (Basel, Switzerland)* **23**, 3360.
487 (DOI:10.3390/molecules23123360).

488 [9] Thorpe, W. H. 1939 Further studies on pre-imaginal olfactory conditioning in insects.
489 *Proceedings of the Royal Society B* **127**, 424-433. (DOI:10.1098/rspb.1939.0032).

490 [10] J. Rice, P. & Coats, J. 1994 *Insecticidal Properties of Several Monoterpenoids to the*
491 *House Fly (Diptera: Muscidae), Red Flour Beetle (Coleoptera: Tenebrionidae), and*
492 *Southern Corn Rootworm (Coleoptera: Chrysomelidae)*1172-1179 p.

493 [11] Samarasekera, R., Weerasinghe Indira, S. & Hemalal, K. D. P. 2007 Insecticidal activity
494 of menthol derivatives against mosquitoes. *Pest Management Science* **64**, 290-295.
495 (DOI:10.1002/ps.1516).

496 [12] Bandell, M., Dubin, A. E., Petrus, M. J., Orth, A., Mathur, J., Hwang, S. W. &
497 Patapoutian, A. 2006 High-throughput random mutagenesis screen reveals TRPM8
498 residues specifically required for activation by menthol. *Nature Neuroscience* **9**, 493.
499 (DOI:10.1038/nn1665).

500 [13] Janssens, A. & Voets, T. 2011 Ligand stoichiometry of the cold- and menthol-activated
501 channel TRPM8. *The Journal of Physiology* **589**, 4827-4835.
502 (DOI:doi:10.1113/jphysiol.2011.216523).

503 [14] Malkia, A., Pertusa, M., Fernández-Ballester, G., Ferrer-Montiel, A. & Viana, F. 2009
504 Differential Role of the Menthol-Binding Residue Y745 in the Antagonism of Thermally
505 Gated TRPM8 Channels. *Molecular Pain* **5**, 1744-8069-1745-1762. (DOI:10.1186/1744-
506 8069-5-62).

507 [15] Myers, B. R., Sigal, Y. M. & Julius, D. 2009 Evolution of thermal response properties in
508 a cold-activated TRP channel. *PloS one* **4**, e5741-e5741.
509 (DOI:10.1371/journal.pone.0005741).

510 [16] Pedretti, A., Marconi, C., Bettinelli, I. & Vistoli, G. 2009 Comparative modeling of the
511 quaternary structure for the human TRPM8 channel and analysis of its binding features.
512 *Biochimica et Biophysica Acta (BBA) - Biomembranes* **1788**, 973-982.
513 (DOI:https://doi.org/10.1016/j.bbamem.2009.02.007).

514 [17] Peier, A. M., Moqrich, A., Hergarden, A. C., Reeve, A. J., Andersson, D. A., Story, G.
515 M., Earley, T. J., Dragoni, I., McIntyre, P., Bevan, S., et al. 2002 A TRP Channel that
516 Senses Cold Stimuli and Menthol. *Cell* **108**, 705-715. (DOI:https://doi.org/10.1016/S0092-
517 8674(02)00652-9).

518 [18] Pertusa, M., Rivera, B., González, A., Ugarte, G. & Madrid, R. 2018 Critical role of the
519 pore domain in the cold response of TRPM8 channels identified by ortholog functional
520 comparison. *Journal of Biological Chemistry* **293**, 12454-12471.
521 (DOI:10.1074/jbc.RA118.002256).

522 [19] Rath, P., Hilton, J. K., Sisco, N. J. & Van Horn, W. D. 2016 Implications of Human
523 Transient Receptor Potential Melastatin 8 (TRPM8) Channel Gating from Menthol Binding
524 Studies of the Sensing Domain. *Biochemistry* **55**, 114-124.
525 (DOI:10.1021/acs.biochem.5b00931).

526 [20] Yin, Y., Wu, M., Zubcevic, L., Borschel, W. F., Lander, G. C. & Lee, S.-Y. 2018
527 Structure of the cold- and menthol-sensing ion channel TRPM8. *Science* **359**, 237-241.
528 (DOI:10.1126/science.aan4325).

529 [21] Karashima, Y., Damann, N., Prenen, J., Talavera, K., Segal, A., Voets, T. & Nilius, B.
530 2007 Bimodal Action of Menthol on the Transient Receptor Potential Channel TRPA1. *The
531 Journal of Neuroscience* **27**, 9874.

532 [22] McKemy, D. D., Neuhausser, W. M. & Julius, D. 2002 Identification of a cold receptor
533 reveals a general role for TRP channels in thermosensation. *Nature* **416**, 52.
534 (DOI:10.1038/nature719).

535 [23] Macpherson, L. J., Dubin, A. E., Evans, M. J., Marr, F., Schultz, P. G., Cravatt, B. F. &
536 Patapoutian, A. 2007 Noxious compounds activate TRPA1 ion channels through covalent
537 modification of cysteines. *Nature* **445**, 541. (DOI:10.1038/nature05544).

538 [24] Story, G. M., Peier, A. M., Reeve, A. J., Eid, S. R., Mosbacher, J., Hricik, T. R., Earley,
539 T. J., Hergarden, A. C., Andersson, D. A., Hwang, S. W., et al. 2003 ANKTM1, a TRP-like
540 Channel Expressed in Nociceptive Neurons, Is Activated by Cold Temperatures. *Cell* **112**,
541 819-829. (DOI:https://doi.org/10.1016/S0092-8674(03)00158-2).

542 [25] Saito, S. & Shingai, R. 2006 Evolution of thermoTRP ion channel homologs in
543 vertebrates. *Physiological Genomics* **27**, 219-230.
544 (DOI:10.1152/physiolgenomics.00322.2005).

545 [26] Dhaka, A., Murray, A. N., Mathur, J., Earley, T. J., Petrus, M. J. & Patapoutian, A. 2007
546 TRPM8 Is Required for Cold Sensation in Mice. *Neuron* **54**, 371-378.
547 (DOI:https://doi.org/10.1016/j.neuron.2007.02.024).

548 [27] Kang, K., Pulver, S. R., Panzano, V. C., Chang, E. C., Griffith, L. C., Theobald, D. L. &
549 Garrity, P. A. 2010 Analysis of *Drosophila* TRPA1 reveals an ancient origin for human
550 chemical nociception. *Nature* **464**, 597. (DOI:10.1038/nature08848).

551 [28] Peng, G., Shi, X. & Kadowaki, T. 2015 Evolution of TRP channels inferred by their
552 classification in diverse animal species. *Molecular Phylogenetics and Evolution* **84**, 145-157.
553 (DOI:https://doi.org/10.1016/j.ympev.2014.06.016).

554 [29] Jordt, S.-E., Bautista, D. M., Chuang, H.-h., McKemy, D. D., Zygmunt, P. M., Högestätt,
555 E. D., Meng, I. D. & Julius, D. 2004 Mustard oils and cannabinoids excite sensory nerve
556 fibres through the TRP channel ANKTM1. *Nature* **427**, 260. (DOI:10.1038/nature02282).

557 [30] Vandewauw, I., De Clercq, K., Mulier, M., Held, K., Pinto, S., Van Ranst, N., Segal, A.,
558 Voet, T., Vennekens, R., Zimmermann, K., et al. 2018 A TRP channel trio mediates acute
559 noxious heat sensing. *Nature* **555**, 662. (DOI:10.1038/nature26137).

560 [31] Xiao, B., Dubin, A. E., Bursulaya, B., Viswanath, V., Jegla, T. J. & Patapoutian, A. 2008
561 Identification of the Transmembrane Domain Five as a Critical Molecular Determinant of
562 Menthol Sensitivity in Mammalian TRPA1 Channels. *The Journal of neuroscience : the*
563 *official journal of the Society for Neuroscience* **28**, 9640-9651.
564 (DOI:10.1523/JNEUROSCI.2772-08.2008).

565 [32] Matsuura, H., Sokabe, T., Kohno, K., Tominaga, M. & Kadowaki, T. 2009 Evolutionary
566 conservation and changes in insect TRP channels. *BMC Evolutionary Biology* **9**, 228-228.
567 (DOI:10.1186/1471-2148-9-228).

568 [33] Turner, H. N., Armengol, K., Patel, A. A., Himmel, N. J., Sullivan, L., Iyer, S. C.,
569 Bhattacharya, S., Iyer, E. P. R., Landry, C., Galko, M. J., et al. 2016 The TRP Channels
570 Pkd2, NompC, and Trpm Act in Cold-Sensing Neurons to Mediate Unique Aversive
571 Behaviors to Noxious Cold in *Drosophila*. *Current Biology* **26**, 3116-3128.
572 (DOI:10.1016/j.cub.2016.09.038).

573 [34] Himmel, N. J., Patel, A. A. & Cox, D. N. 2017 Invertebrate Nociception. *The Oxford*
574 *Research Encyclopedia of Neuroscience*. (DOI:10.1093/acrefore/9780190264086.013.166).

575 [35] Kim, S. H., Lee, Y., Akitake, B., Woodward, O. M., Guggino, W. B. & Montell, C. 2010
576 *Drosophila* TRPA1 channel mediates chemical avoidance in gustatory receptor neurons.
577 *Proceedings of the National Academy of Sciences* **107**, 8440.

578 [36] Neely, G. G., Keene, A. C., Duchek, P., Chang, E. C., Wang, Q.-P., Aksoy, Y. A.,
579 Rosenzweig, M., Costigan, M., Woolf, C. J., Garrity, P. A., et al. 2011 TrpA1 Regulates
580 Thermal Nociception in *Drosophila*. *PLOS ONE* **6**, e24343.
581 (DOI:10.1371/journal.pone.0024343).

582 [37] Zhong, L., Bellemer, A., Yan, H., Honjo, K., Robertson, J., Hwang, Richard Y., Pitt,
583 Geoffrey S. & Tracey, W. D. 2012 Thermosensory and Nonthermosensory Isoforms of
584 Drosophila melanogaster TRPA1 Reveal Heat-Sensor Domains of a ThermoTRP Channel.
585 *Cell Reports* **1**, 43-55. (DOI:https://doi.org/10.1016/j.celrep.2011.11.002).

586 [38] Peng, G., Kashio, M., Li, T., Dong, X., Tominaga, M. & Kadowaki, T. 2016 TRPA1
587 Channels in *Drosophila* and Honey Bee Ectoparasitic Mites Share Heat Sensitivity and

14

588 Temperature-Related Physiological Functions. *Frontiers in physiology* **7**, 447-447.
589 (DOI:10.3389/fphys.2016.00447).

590 [39] Wang, X., Li, T., Kashio, M., Xu, Y., Tominaga, M. & Kadowaki, T. 2018 HsTRPA of the
591 Red Imported Fire Ant, *Solenopsis invicta*, Functions as a Nocisensor and Uncovers the
592 Evolutionary Plasticity of HsTRPA Channels. *eNeuro* **5**, ENEURO.0327-0317.2018.
593 (DOI:10.1523/ENEURO.0327-17.2018).

594 [40] Gracheva, E. O., Ingolia, N. T., Kelly, Y. M., Cordero-Morales, J. F., Hollopeter, G.,
595 Chesler, A. T., Sánchez, E. E., Perez, J. C., Weissman, J. S. & Julius, D. 2010 Molecular
596 basis of infrared detection by snakes. *Nature* **464**, 1006. (DOI:10.1038/nature08943).

597 [41] Moparthi, L., Kichko, T. I., Eberhardt, M., Högestätt, E. D., Kjellbom, P., Johanson, U.,
598 Reeh, P. W., Leffler, A., Filipovic, M. R. & Zygmunt, P. M. 2016 Human TRPA1 is a heat
599 sensor displaying intrinsic U-shaped thermosensitivity. *Scientific Reports* **6**, 28763.
600 (DOI:10.1038/srep28763).

601 [42] Saito, C. T., Fukuta, N., Tominaga, M., Saito, S., Ohta, T., Takahashi, K., Banzawa, N.
602 & Imagawa, T. 2014 Heat and Noxious Chemical Sensor, Chicken TRPA1, as a Target of
603 Bird Repellents and Identification of Its Structural Determinants by Multispecies Functional
604 Comparison. *Molecular Biology and Evolution* **31**, 708-722. (DOI:10.1093/molbev/msu001).

605 [43] Saito, S., Nakatsuka, K., Takahashi, K., Fukuta, N., Imagawa, T., Ohta, T. & Tominaga,
606 M. 2012 Analysis of transient receptor potential ankyrin 1 (TRPA1) in frogs and lizards
607 illuminates both nociceptive heat and chemical sensitivities and coexpression with TRP
608 vanilloid 1 (TRPV1) in ancestral vertebrates. *The Journal of biological chemistry* **287**,
609 30743-30754. (DOI:10.1074/jbc.M112.362194).

610 [44] Sato, A., Sokabe, T., Kashio, M., Yasukochi, Y., Tominaga, M. & Shiomi, K. 2014
611 Embryonic thermosensitive TRPA1 determines transgenerational diapause phenotype of
612 the silkworm, Bombyx mori. *Proceedings of the National Academy of Sciences of the United*
613 *States of America* **111**, E1249-E1255. (DOI:10.1073/pnas.1322134111).

614 [45] Wang, G., Qiu, Y. T., Lu, T., Kwon, H.-W., Pitts, R. J., Van Loon, J. J. A., Takken, W. &
615 Zwiebel, L. J. 2009 *Anopheles gambiae* TRPA1 is a heat-activated channel expressed in
616 thermosensitive sensilla of female antennae. *The European journal of neuroscience* **30**,
617 967-974. (DOI:10.1111/j.1460-9568.2009.06901.x).

618 [46] Caspani, O. & Heppenstall, P. A. 2009 TRPA1 and cold transduction: an unresolved
619 issue? *The Journal of general physiology* **133**, 245-249. (DOI:10.1085/jgp.200810136).

620 [47] Chen, J., Kang, D., Xu, J., Lake, M., Hogan, J. O., Sun, C., Walter, K., Yao, B. & Kim,
621 D. 2013 Species differences and molecular determinant of TRPA1 cold sensitivity. *Nature*
622 *communications* **4**, 2501-2501. (DOI:10.1038/ncomms3501).

623 [48] Saito, S. & Tominaga, M. 2017 Evolutionary tuning of TRPA1 and TRPV1 thermal and
624 chemical sensitivity in vertebrates. *Temperature (Austin, Tex.)* **4**, 141-152.
625 (DOI:10.1080/23328940.2017.1315478).

626 [49] Walters, E. T. 2018 Nociceptive Biology of Molluscs and Arthropods: Evolutionary
627 Clues About Functions and Mechanisms Potentially Related to Pain. *Frontiers in physiology*
628 **9**, 1049-1049. (DOI:10.3389/fphys.2018.01049).

629 [50] Im, S. H., Patel, A. A., Cox, D. N. & Galko, M. J. 2018 *Drosophila* Insulin receptor
630 regulates the persistence of injury-induced nociceptive sensitization. *Disease Models*
631 *&amp; Mechanisms* **11**, dmm034231. (DOI:10.1242/dmm.034231).

632 [51] Patel, A. A. & Cox, D. N. 2017 Behavioral and Functional Assays for Investigating
633 Mechanisms of Noxious Cold Detection and Multimodal Sensory Processing in Drosophila
634 Larvae. *Bio-protocol* **7**, e2388. (DOI:10.21769/BioProtoc.2388).

635 [52] Kozma, M. T., Schmidt, M., Ngo-Vu, H., Sparks, S. D., Senatore, A. & Derby, C. D.
636 2018 Chemoreceptor proteins in the Caribbean spiny lobster, *Panulirus argus*: Expression
637 of Ionotropic Receptors, Gustatory Receptors, and TRP channels in two chemosensory
638 organs and brain. *PloS one* **13**, e0203935-e0203935. (DOI:10.1371/journal.pone.0203935).

639 [53] Shinzato, C., Shoguchi, E., Kawashima, T., Hamada, M., Hisata, K., Tanaka, M., Fujie,
640 M., Fujiwara, M., Koyanagi, R., Ikuta, T., et al. 2011 Using the *Acropora digitifera* genome to
641 understand coral responses to environmental change. *Nature* **476**, 320.
642 (DOI:10.1038/nature10249).

643 [54] Kudtarkar, P. & Cameron, R. A. 2017 Echinobase: an expanding resource for
644 echinoderm genomic information. *Database* **2017**. (DOI:10.1093/database/bax074).

645 [55] Yuan, A., He, D., Davidson, E., Samanta, M. & Cameron, R. A. 2008 SpBase: the sea
646 urchin genome database and web site. *Nucleic Acids Research* **37**, D750-D754.
647 (DOI:10.1093/nar/gkn887).

648 [56] Albertin, C. B., Simakov, O., Mitros, T., Wang, Z. Y., Pungor, J. R., Edsinger-Gonzales,
649 E., Brenner, S., Ragsdale, C. W. & Rokhsar, D. S. 2015 The octopus genome and the
650 evolution of cephalopod neural and morphological novelties. *Nature* **524**, 220.
651 (DOI:10.1038/nature14668).

652 [57] Altschul, S. F., Madden, T. L., Schäffer, A. A., Zhang, J., Zhang, Z., Miller, W. &
653 Lipman, D. J. 1997 Gapped BLAST and PSI-BLAST: a new generation of protein database
654 search programs. *Nucleic acids research* **25**, 3389-3402.

655 [58] Jones, P., Binns, D., Chang, H.-Y., Fraser, M., Li, W., McAnulla, C., McWilliam, H.,
656 Maslen, J., Mitchell, A., Nuka, G., et al. 2014 InterProScan 5: genome-scale protein function
657 classification. *Bioinformatics (Oxford, England)* **30**, 1236-1240.
658 (DOI:10.1093/bioinformatics/btu031).

659 [59] Edgar, R. C. 2004 MUSCLE: multiple sequence alignment with high accuracy and high
660 throughput. *Nucleic acids research* **32**, 1792-1797. (DOI:10.1093/nar/gkh340).

661 [60] Stecher, G., Kumar, S. & Tamura, K. 2016 MEGA7: Molecular Evolutionary Genetics
662 Analysis Version 7.0 for Bigger Datasets. *Molecular Biology and Evolution* **33**, 1870-1874.
663 (DOI:10.1093/molbev/msw054).

664 [61] Capella-Gutiérrez, S., Silla-Martínez, J. M. & Gabaldón, T. 2009 trimAl: a tool for
665 automated alignment trimming in large-scale phylogenetic analyses. *Bioinformatics (Oxford,*
666 *England)* **25**, 1972-1973. (DOI:10.1093/bioinformatics/btp348).

667 [62] Schmidt, H. A., Minh, B. Q., von Haeseler, A. & Nguyen, L.-T. 2014 IQ-TREE: A Fast
668 and Effective Stochastic Algorithm for Estimating Maximum-Likelihood Phylogenies.
669 *Molecular Biology and Evolution* **32**, 268-274. (DOI:10.1093/molbev/msu300).

[63] Goldman, N. & Parks, S. L. 2014 Maximum Likelihood Inference of Small Trees in the Presence of Long Branches. *Systematic Biology* **63**, 798-811. (DOI:10.1093/sysbio/syu044).

[64] Kück, P., Mayer, C., Wägele, J.-W. & Misof, B. 2012 Long Branch Effects Distort Maximum Likelihood Phylogenies in Simulations Despite Selection of the Correct Model. *PLOS ONE* **7**, e36593. (DOI:10.1371/journal.pone.0036593).

[65] Philippe, H., Zhou, Y., Brinkmann, H., Rodrigue, N. & Delsuc, F. 2005 Heterotachy and long-branch attraction in phylogenetics. *BMC evolutionary biology* **5**, 50-50. (DOI:10.1186/1471-2148-5-50).

[66] Huelsenbeck, J. P., Ronquist, F., Nielsen, R. & Bollback, J. P. 2001 Bayesian Inference of Phylogeny and Its Impact on Evolutionary Biology. *Science* **294**, 2310-2314. (DOI:10.1126/science.1065889).

[67] Ronquist, F. & Huelsenbeck, J. P. 2003 MrBayes 3: Bayesian phylogenetic inference under mixed models. *Bioinformatics* **19**, 1572-1574. (DOI:10.1093/bioinformatics/btg180).

[68] Kalyaanamoorthy, S., Minh, B. Q., Wong, T. K. F., von Haeseler, A. & Jermiin, L. S. 2017 ModelFinder: fast model selection for accurate phylogenetic estimates. *Nature Methods* **14**, 587. (DOI:10.1038/nmeth.4285).

[69] Hoang, D. T., Vinh, L. S., Chernomor, O., Minh, B. Q. & von Haeseler, A. 2017 UFBoot2: Improving the Ultrafast Bootstrap Approximation. *Molecular Biology and Evolution* **35**, 518-522. (DOI:10.1093/molbev/msx281).

[70] Letunic, I. & Bork, P. 2016 Interactive tree of life (iTOL) v3: an online tool for the display and annotation of phylogenetic and other trees. *Nucleic acids research* **44**, W242-W245. (DOI:10.1093/nar/gkw290).

[71] Thornton, J. M., Jones, D. T. & Taylor, W. R. 1992 The rapid generation of mutation data matrices from protein sequences. *Bioinformatics* **8**, 275-282. (DOI:10.1093/bioinformatics/8.3.275).

[72] Lenth, R. V. 2016 Least-Squares Means: The R Package lsmeans. *2016* **69**, 33. (DOI:10.18637/jss.v069.i01).

[73] Hwang, R. Y., Zhong, L., Xu, Y., Johnson, T., Zhang, F., Deisseroth, K. & Tracey, W. D. 2007 Nociceptive neurons protect *Drosophila* larvae from parasitoid wasps. *Current biology : CB* **17**, 2105-2116. (DOI:10.1016/j.cub.2007.11.029).

[74] Tracey, W. D., Wilson, R. I., Laurent, G. & Benzer, S. 2003 *painless*, a *Drosophila* Gene Essential for Nociception. *Cell* **113**, 261-273. (DOI:https://doi.org/10.1016/S0092-8674(03)00272-1).

[75] Im, S. H. & Galko, M. J. 2012 Pokes, sunburn, and hot sauce: *Drosophila* as an emerging model for the biology of nociception. *Developmental dynamics : an official publication of the American Association of Anatomists* **241**, 16-26. (DOI:10.1002/dvdy.22737).

[76] Tsubouchi, A., Caldwell, J. C. & Tracey, W. D. 2012 Dendritic filopodia, Ripped Pocket, NOMPC, and NMDARs contribute to the sense of touch in *Drosophila* larvae. *Current biology : CB* **22**, 2124-2134. (DOI:10.1016/j.cub.2012.09.019).

[77] Xiang, Y., Yuan, Q., Vogt, N., Looger, L. L., Jan, L. Y. & Jan, Y. N. 2010 Light-avoidance-mediating photoreceptors tile the *Drosophila* larval body wall. *Nature* **468**, 921. (DOI:10.1038/nature09576).

[78] Yan, Z., Zhang, W., He, Y., Gorczyca, D., Xiang, Y., Cheng, L. E., Meltzer, S., Jan, L. Y. & Jan, Y. N. 2013 Drosophila NOMPC is a mechanotransduction channel subunit for gentle-touch sensation. *Nature* **493**, 221-225. (DOI:10.1038/nature11685).

[79] Fosque, B. F., Sun, Y., Dana, H., Yang, C.-T., Ohyama, T., Tadross, M. R., Patel, R., Zlatic, M., Kim, D. S., Ahrens, M. B., et al. 2015 Labeling of active neural circuits in vivo with designed calcium integrators. *Science* **347**, 755. (DOI:10.1126/science.1260922).

[80] Iyer, E. P. R., Iyer, S. C., Sullivan, L., Wang, D., Meduri, R., Graybeal, L. L. & Cox, D. N. 2013 Functional genomic analyses of two morphologically distinct classes of *Drosophila* sensory neurons: post-mitotic roles of transcription factors in dendritic patterning. *PloS one* **8**, e72434-e72434. (DOI:10.1371/journal.pone.0072434).

[81] Driscoll, K., Stanfield, G. M., Droste, R. & Horvitz, H. R. 2017 Presumptive TRP channel CED-11 promotes cell volume decrease and facilitates degradation of apoptotic cells in *Caenorhabditis elegans*. *Proceedings of the National Academy of Sciences* **114**, 8806-8811. (DOI:10.1073/pnas.1705084114).

[82] Arenas, O. M., Zaharieva, E. E., Para, A., Vásquez-Doorman, C., Petersen, C. P. & Gallio, M. 2017 Activation of planarian TRPA1 by reactive oxygen species reveals a conserved mechanism for animal nociception. *Nature Neuroscience* **20**, 1686-1693. (DOI:10.1038/s41593-017-0005-0).

[83] Chatzigeorgiou, M., Yoo, S., Watson, J. D., Lee, W.-H., Spencer, W. C., Kindt, K. S., Hwang, S. W., Miller Iii, D. M., Treinin, M., Driscoll, M., et al. 2010 Specific roles for DEG/ENaC and TRP channels in touch and thermosensation in *C. elegans* nociceptors. *Nature Neuroscience* **13**, 861. (DOI:10.1038/nn.2581).

[84] Doerner, J. F., Gisselmann, G., Hatt, H. & Wetzel, C. H. 2007 Transient Receptor Potential Channel A1 Is Directly Gated by Calcium Ions. *Journal of Biological Chemistry* **282**, 13180-13189. (DOI:10.1074/jbc.M607849200).

[85] Sawada, Y., Hosokawa, H., Hori, A., Matsumura, K. & Kobayashi, S. 2007 Cold sensitivity of recombinant TRPA1 channels. *Brain Res* **1160**, 39-46. (DOI:10.1016/j.brainres.2007.05.047).

[86] Zurborg, S., Yurgionas, B., Jira, J. A., Caspani, O. & Heppenstall, P. A. 2007 Direct activation of the ion channel TRPA1 by Ca2+. *Nature Neuroscience* **10**, 277. (DOI:10.1038/nn1843).

[87] Gaudioso, C., Hao, J., Martin-Eauclaire, M.-F., Gabriac, M. & Delmas, P. 2012 Menthol pain relief through cumulative inactivation of voltage-gated sodium channels. *PAIN* **153**, 473-484. (DOI:10.1016/j.pain.2011.11.014).

[88] Macpherson, L. J., Hwang, S. W., Miyamoto, T., Dubin, A. E., Patapoutian, A. & Story, G. M. 2006 More than cool: Promiscuous relationships of menthol and other sensory compounds. *Molecular and Cellular Neuroscience* **32**, 335-343. (DOI:https://doi.org/10.1016/j.mcn.2006.05.005).

[89] Morise, M., Ito, Y., Matsuno, T., Hibino, Y., Mizutani, T., Ito, S., Hashimoto, N., Kondo, M., Imaizumi, K. & Hasegawa, Y. 2010 Heterologous regulation of anion transporters by

753 menthol in human airway epithelial cells. *European Journal of Pharmacology* **635**, 204-211.
754 (DOI:https://doi.org/10.1016/j.ejphar.2010.03.032).

755 [90] Oz, M., El Nebrisi, E. G., Yang, K.-H. S., Howarth, F. C. & Al Kury, L. T. 2017 Cellular
756 and Molecular Targets of Menthol Actions. *Frontiers in pharmacology* **8**, 472-472.
757 (DOI:10.3389/fphar.2017.00472).

758 [91] Parnas, M., Peters, M., Dadon, D., Lev, S., Vertkin, I., Slutsky, I. & Minke, B. 2009
759 Carvacrol is a novel inhibitor of *Drosophila* TRPL and mammalian TRPM7 channels. *Cell*
760 *calcium* **45**, 300-309. (DOI:10.1016/j.ceca.2008.11.009).

761 [92] Drew, B. T. & Sytsma, K. J. 2012 Phylogenetics, biogeography, and staminal evolution
762 in the tribe Mentheae (Lamiaceae). *American Journal of Botany* **99**, 933-953.
763 (DOI:10.3732/ajb.1100549).

764 [93] Singh, B. & Sharma, R. A. 2015 Plant terpenes: defense responses, phylogenetic
765 analysis, regulation and clinical applications. *3 Biotech* **5**, 129-151. (DOI:10.1007/s13205-
766 014-0220-2).

767 [94] Kühn, F. J. P., Witschas, K., Kühn, C. & Lückhoff, A. 2010 Contribution of the S5-Pore-
768 S6 Domain to the Gating Characteristics of the Cation Channels TRPM2 and TRPM8. *The*
769 *Journal of Biological Chemistry* **285**, 26806-26814. (DOI:10.1074/jbc.M110.109975).

770 [95] Chen, J.-Y., Iten, H. & Cheng, Y.-N. 1997 *The Cambrian explosion and the fossil*
771 *record*, National Museum of Natural Science.

772 [96] Bailly, X., Reichert, H. & Hartenstein, V. 2013 The urbilaterian brain revisited: novel
773 insights into old questions from new flatworm clades. *Development genes and evolution*
774 **223**, 149-157. (DOI:10.1007/s00427-012-0423-7).

775 [97] Hejnol, A. & Martindale, M. Q. 2008 Acoel development supports a simple planula-like
776 urbilaterian. *Philosophical Transactions of the Royal Society B: Biological Sciences* **363**,
777 1493-1501. (DOI:doi:10.1098/rstb.2007.2239).

778 [98] Moroz, L. L. 2009 On the independent origins of complex brains and neurons. *Brain,*
779 *behavior and evolution* **74**, 177-190. (DOI:10.1159/000258665).

780 [99] Moroz, L. L. 2012 Phylogenomics meets neuroscience: how many times might complex
781 brains have evolved? *Acta biologica Hungarica* **63 Suppl 2**, 3-19.
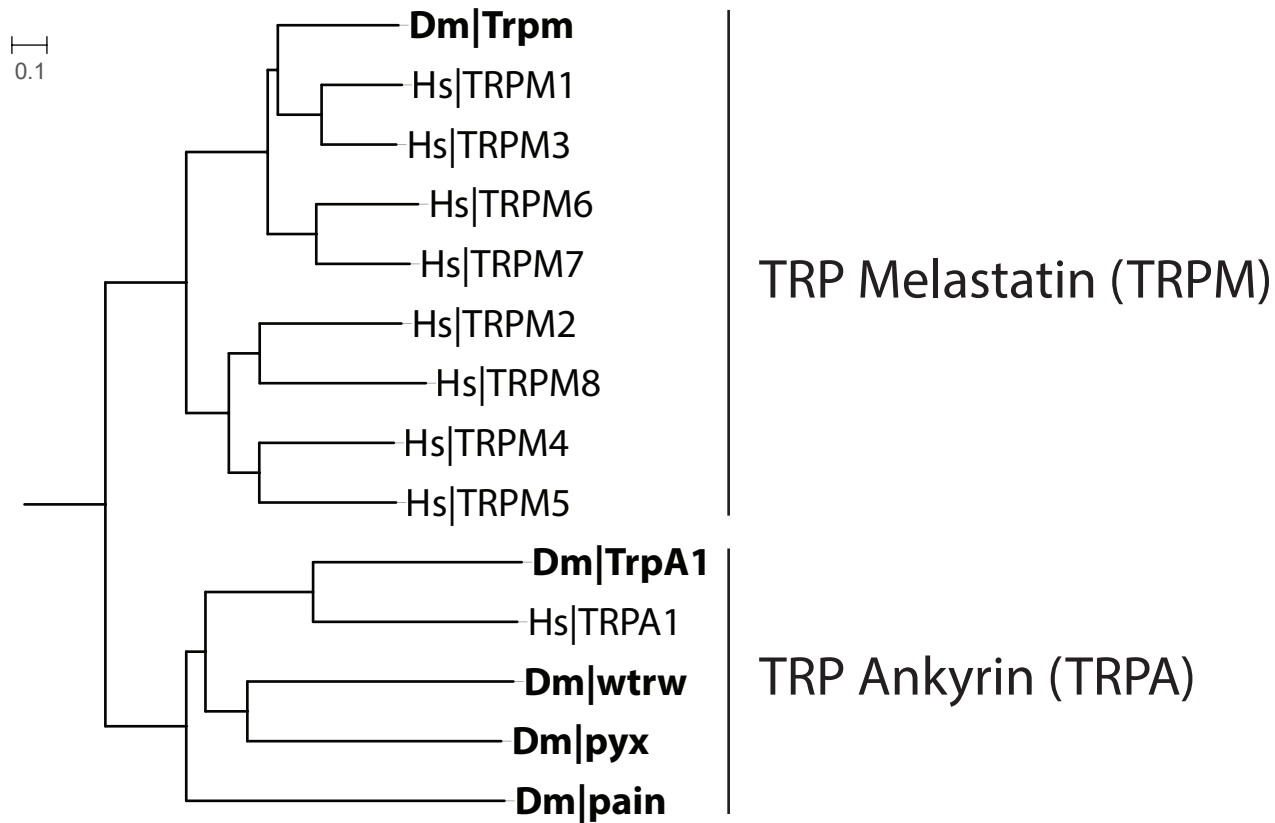782 (DOI:10.1556/ABiol.63.2012.Suppl.2.1).

783 [100] Northcutt, R. G. 2010 Cladistic Analysis Reveals Brainless Urbilateria. *Brain, Behavior*
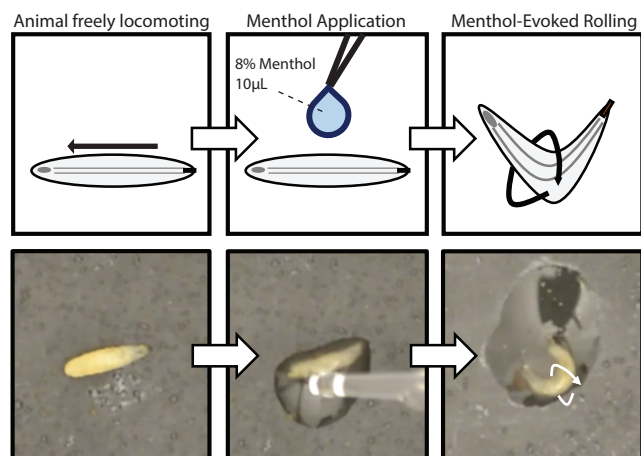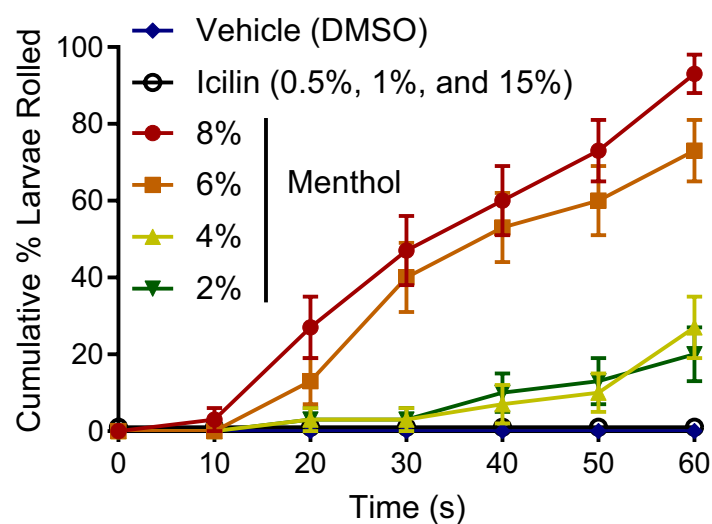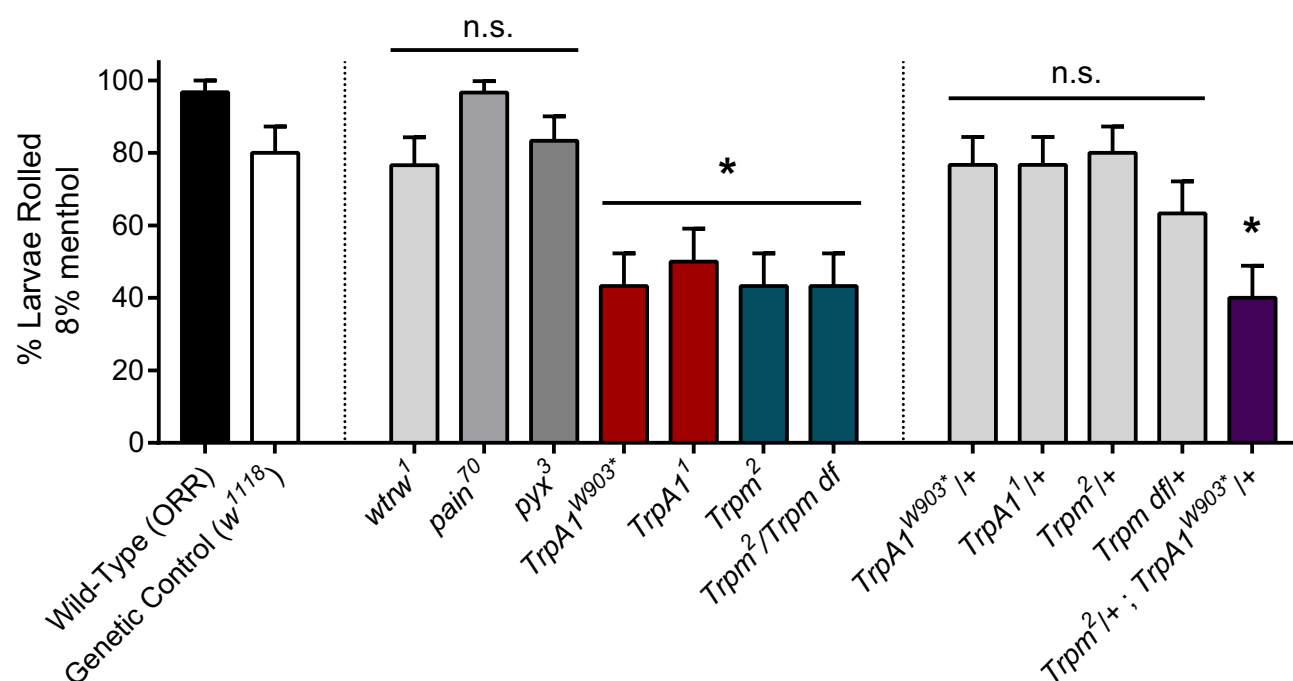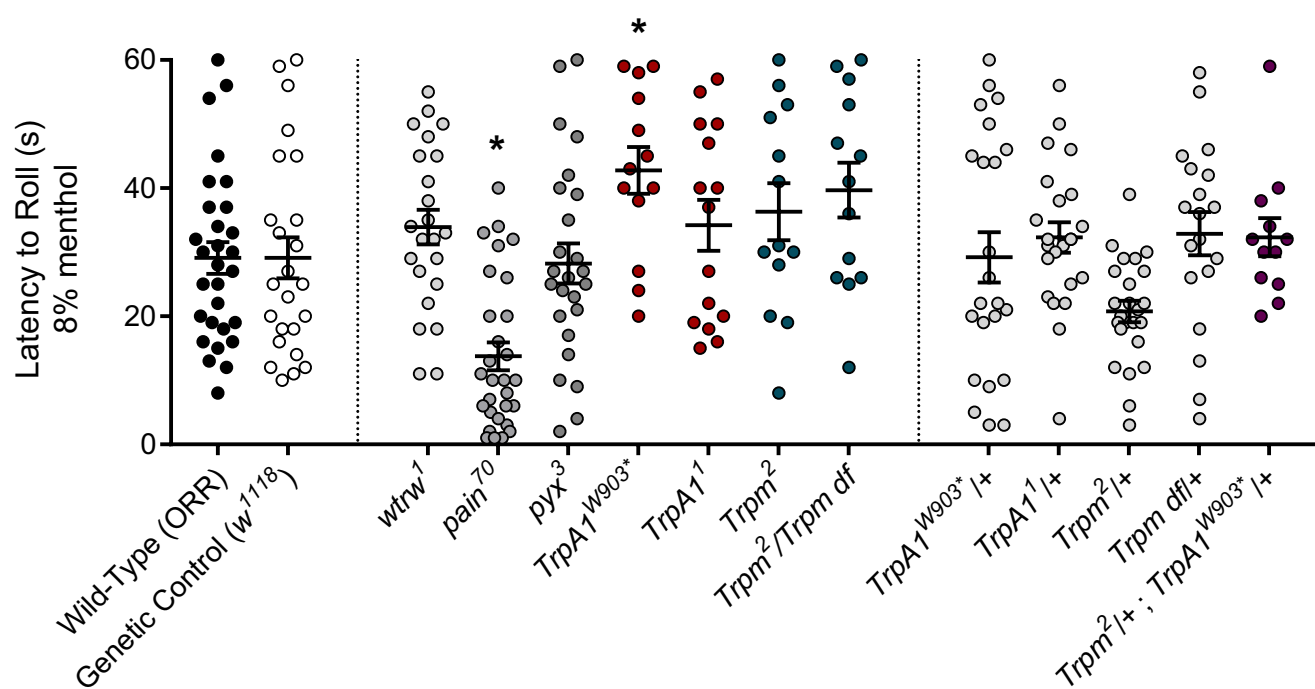784 *and Evolution* **76**, 1-2. (DOI:10.1159/000316443).

785 [101] Schulz-Bohm, K., Martín-Sánchez, L. & Garbeva, P. 2017 Microbial Volatiles: Small
786 Molecules with an Important Role in Intra- and Inter-Kingdom Interactions. *Frontiers in*
787 *Microbiology* **8**. (DOI:10.3389/fmicb.2017.02484).

788 [102] Schmidt, R., Jager, V. d., Zühlke, D., Wolff, C., Bernhardt, J., Cankar, K., Beekwilder,
789 J., Ijcken, W. v., Sleutels, F., Boer, W. d., et al. 2017 Fungal volatile compounds induce
790 production of the secondary metabolite Sodorifen in Serratia plymuthica PRI-2C. *Scientific*
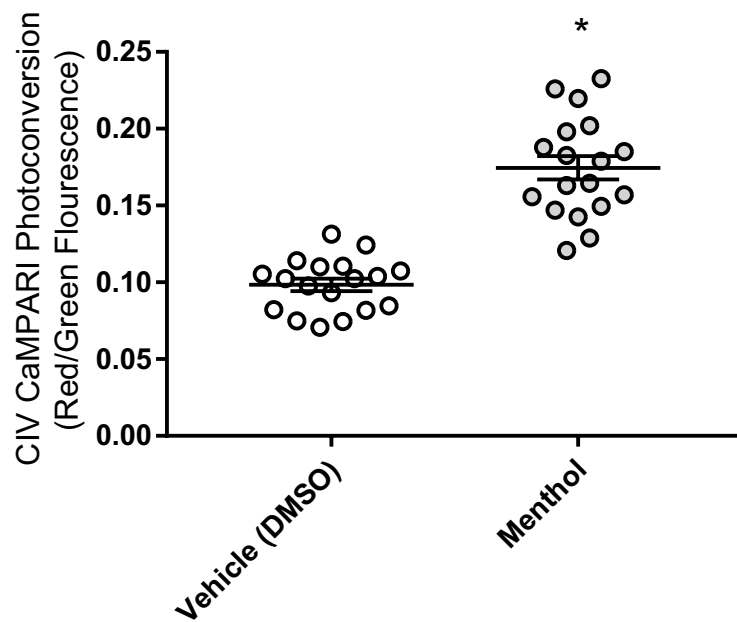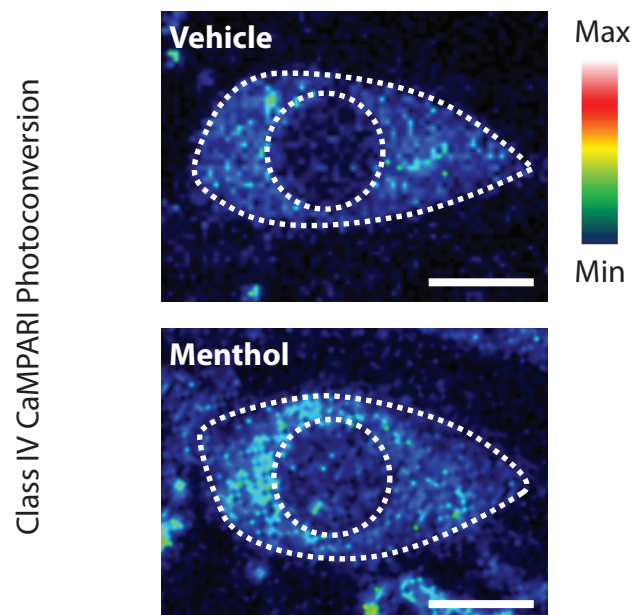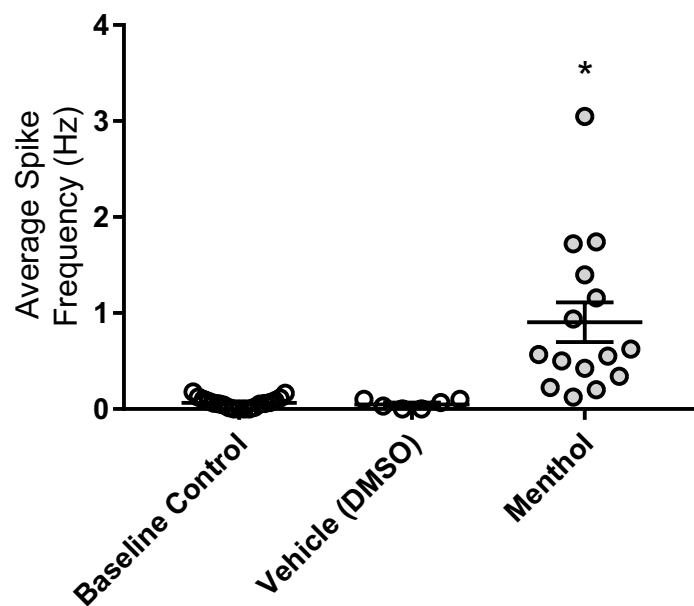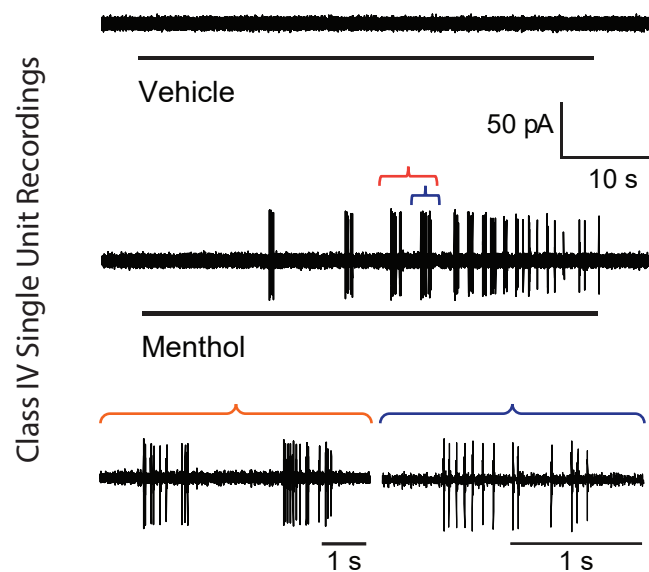791 *Reports* **7**, 862. (DOI:10.1038/s41598-017-00893-3).

Figure 1

Figure 2

Figure 3

Figure 4

Figure 5

A Cladogram

Species	TRPM Basal	TRPM α	TRPM β	TRPA TRPA1	TRPA Other
Monosiga brevicollis (Chaonoflagellate, Mb)	3	-	-	-	2
Hydra vulgaris (Fresh-water polyp, Hv)	-	3	-	-	4
Acropora digitifera (Coral, Ad)	-	1	1	-	10
Nematostella vectensis (Starlet sea anemone, Nv)	-	2	1	-	2
Strongylocentrotus purpuratus (Purple sea urchin, Sp)	-	1	-	-	1
Danio rerio (Zebrafish, Dr)	-	5	6	2	-
Gallus gallus (Red junglefowl, or chicken, Gg)	-	4	3	1	-
Mus musculus (Mouse, Mm)	-	4	4	1	-
Homo sapiens (Human, Hs)	-	4	4	1	-
Aplysia californica (California sea hare, Ac)	1	2	1	2	1
Octopus bimaculoides (California two-spot octopus, Ob)	-	1	2	1	1
Priapulus caudatus (Priapulid worm, Pc)	1	1	2	-	1
Caenorhabditis elegans (Nematode, Ce)*	1	3	-	-	1
Galendromus occidentalis (Western predatory mite, Go)	1	-	-	1	-
Strigamia maritima (Centipede, Sm)	2	-	-	2	1
Apis mellifera (European Honey Bee, Am)	-	1	-	-	4
Drosophila melanogaster (Common fruit fly, Dm)	-	1	-	1	3
Panulirus argus (Carribean spiny lobster, Pa)*	-	1	-	-	7
Daphnia pulex (Water flea, Dp)	-	2	-	-	5

Ancestral Bilaterian (AB)

Critical Structures

TRPM

TRPA1